Transverse-momentum spectrum of inclusive reactions in the geometrical picture

S. Y. Lo and Li Yang-guo*
School of Physics, University of Melbourne, Parkville, Victoria 3052, Australia
(Received 1 December 1982)

The geometrical model of hadron elastic scattering is generalized to encompass the transverse-momentum spectrum of inclusive reactions. The model is capable of explaining the rapidly rising cross section at large momentum transfer squared as a result of the rising total cross section. We fit all data from $\sqrt{s} \cong 5$ to 540 GeV and from $P_t^2 = 0$ to 25 GeV^2.

I. INTRODUCTION

Chou and Yang in 1980 investigated the dip and kink structures in hadron-nucleus and hadron-hadron diffraction dissociation.[1] They found that the position of dips or shoulders discovered in the processes

$$\begin{aligned}
&\pi^- A \rightarrow (\pi\pi\pi)A, \text{ for } A = \text{Cu or Pb} ,\\
&pp \rightarrow p(n\pi^+) ,\\
&pp \rightarrow (p\pi^+\pi^-)(p\pi^+\pi^-) ,\\
&np \rightarrow (p\pi^-)p ,\\
&pn \rightarrow (p\pi^+\pi^-)(p\pi^-) ,\\
&nn \rightarrow (p\pi^-)(p\pi^-)
\end{aligned} \tag{1.1}$$

by experiments can be explained by a simple extension of the Chou-Yang model in the geometrical picture.[2–5] For elastic scattering in the Chou-Yang model, the scattering amplitude is given to be

$$1 - e^{\Omega} . \tag{1.2}$$

For the first-order process such as those depicted in (1.1) the scattering amplitude for diffraction scattering is found to be correctly given by

$$\Omega(b)e^{-\Omega(b)} . \tag{1.3}$$

Chou and Yang[1] regarded the hadrons inside parentheses in (1.1) as one object in the final states. In other words they treated the reactions (1.1) as $pp \rightarrow pp^+$, where p^+ is some excited state of proton which subsequently decays into $p^+ \rightarrow n\pi^+, p\pi^+\pi^-$, etc.

It is most interesting to investigate the higher-order terms beyond that of Eq. (1.3). We suggest that they manifest themselves in inclusive reactions such as

$$pp \rightarrow \pi + \text{anything} , \tag{1.4}$$

where it is assumed that the pion arises from a sum total of all pions in the decay of p^+. We find that a good fit can be obtained with data ranging from low energy to extremely high energy.

II. PHYSICAL PICTURE

The physical picture is that while one hadron transverses through another hadron at an impact parameter b, the diffraction association may take place at any point P as shown in Fig. 1. The equation becomes

$$\int e^{2i\delta_0(-\infty,z)} P_1(b,z) e^{2i\delta_0'(z,+\infty)} dz , \tag{2.1}$$

where $e^{2i\delta_0}$ is the S matrix for incoming hadrons, and $e^{2i\delta'}$ is the S matrix for outgoing hadrons

$$\begin{aligned}
2i\delta_0(-\infty,\infty) &= -\Omega_0 ,\\
2i\delta_0'(\infty,+\infty) &= -\Omega_0' .
\end{aligned} \tag{2.2}$$

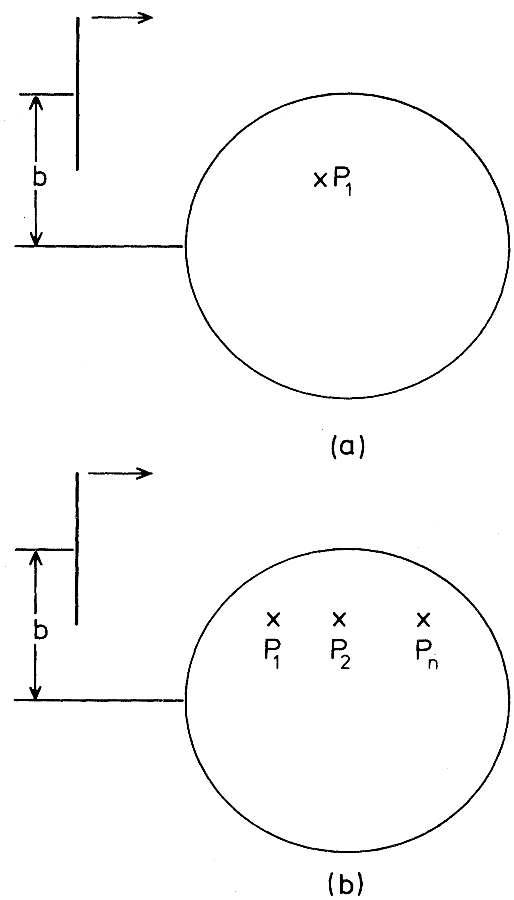

FIG. 1. Schematic diagram for inclusive reactions in geometrical picture; (a) first-order transition at P; (b) higher-order transitions at $P_1, P_2 \cdots P_n$.

The probability of diffractive dissociation occurs all over the target hadron. Hence one has

$$\Omega_1=\int_{-\infty}^{\infty} P_1(b,z)dz \; . \tag{2.3}$$

In general Ω_0,Ω_0' could all be different. The work of Chou and Yang assumes

$$\Omega_0=\Omega_0'=\Omega_1=\Omega \; , \tag{2.4}$$

from which Eq. (1.3) can be easily derived. We argue that this means that in diffractive association of the type

$$pp\rightarrow p^{+}+p \; , \tag{2.5}$$

the transition $p\rightarrow p^{+}$ occurs locally at one single point, and the shape of p^{+} effectively remains the same during the transversal through the target hadron. It expands later and decays, e.g., $p^{+}\rightarrow p(\pi\pi)$ when the two hadrons no longer overlap. To be more concrete, say, hadrons are made up of quarks, quark-antiquark pairs, and gluons. Only the overlapping parts from two hadrons are excited at point P with exchange of energy and momentum and nowhere else. The sharing of energy-momentum throughout the hadron cannot take place faster than the speed of light. If the excitation travels back and forth a few times, the hadrons have already passed through one another. In such a way one can argue that in diffractive dissociation the form factors which produce the overlapping function Ω_0,Ω_0' are similar to those used in elastic scatterings.

The transition expressed in Eqs. (1.3) and (2.1) is for first order. The second-order transition is

$$\frac{1}{2!}\int dz_1 e^{2i\delta_0(-\infty,z_1)}P_1(z_1)e^{2i\delta_0(z_1,z_2)}P_2(z_2)e^{2i\delta_0(z_2,\infty)}dz_2 \tag{2.6}$$

and the nth-order transition is, in general,

$$\frac{1}{n!}\int dz_1\cdots dz_n e^{2i\delta_0(-\infty z_1)}P_1(z_1) \times e^{2i\delta(z_1,z_2)}\cdots P_n(z_n)e^{2i\delta_0(z_n-\infty)} \; . \tag{2.7}$$

Using the same simplification as Eq. (2.2) one reduces (2.6) and (2.7) to

$$\frac{1}{2!}\Omega_1{}^2e^{-\Omega} \; , \qquad \frac{1}{n!}\Omega_1{}^n e^{-\Omega} \; . \tag{2.8}$$

The excited cluster p^{+} in general would be different for first order, second order, or the nth order. Since p^{+} eventually decays into $p^{+}\rightarrow p+\pi+\cdots\pi$, the inclusive reaction $p\rightarrow\pi+X$ can then be regarded as an incoherent sum of all these transitions. For inclusive reactions it is necessary to include other inelastic transitions in the intermediate state other than purely diffractive dissociation. Therefore we would in general have $\Omega_1\neq\Omega_0$, and Ω_1 includes all nonelastic channels that would produce a pion final state.

The above expressions can be derived conveniently from a single formula. We generalize the scattering amplitude to be

$$a(k)=\int(1-S)e^{i\vec{k}\cdot\vec{b}}\frac{d^2b}{(2\pi)} \tag{2.9}$$

with

$$S=\exp(-\Omega_0-\Omega_1) \; , \tag{2.10}$$

where $\Omega_0(b)$ is responsible for the absorption of incoming and outgoing hadrons, and $\Omega_1(b)$ is responsible for the all nonelastic transitions. It is convenient to denote a two-dimensional Fourier transform by

$$(X)_F=\frac{1}{2\pi}\int e^{-i\vec{k}\cdot\vec{b}}X(b)d^2b \; . \tag{2.11}$$

Then the total cross section σ_T and elastic differential cross section are given by

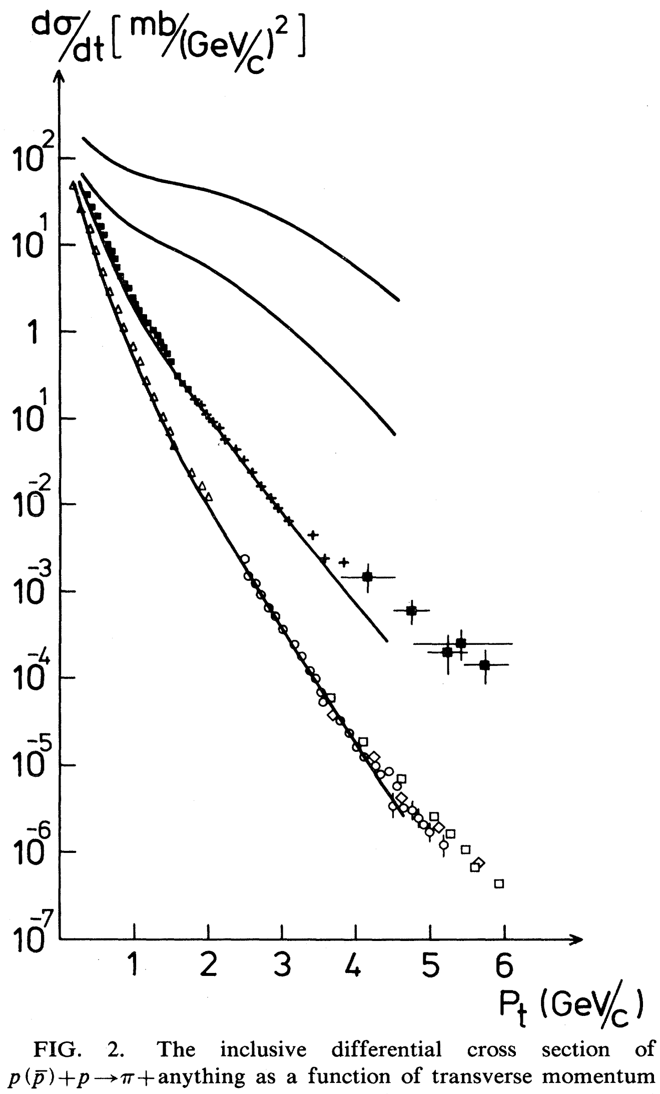

FIG. 2. The inclusive differential cross section of $p(\bar{p})+p\rightarrow\pi+$anything as a function of transverse momentum P_t. Solid lines are theoretical predictions. The experimental points (Ref. 7) are $+$ and ■ for $\bar{p}p$ at $\sqrt{s}=540$ GeV^2, $|y|<2.5$ and $1.6<|y|<2.5$, respectively; △ for pp at $\sqrt{s}=53$ GeV, and at 90°; ◇, ○, and □ for pp at $\sqrt{s}=63$ GeV.

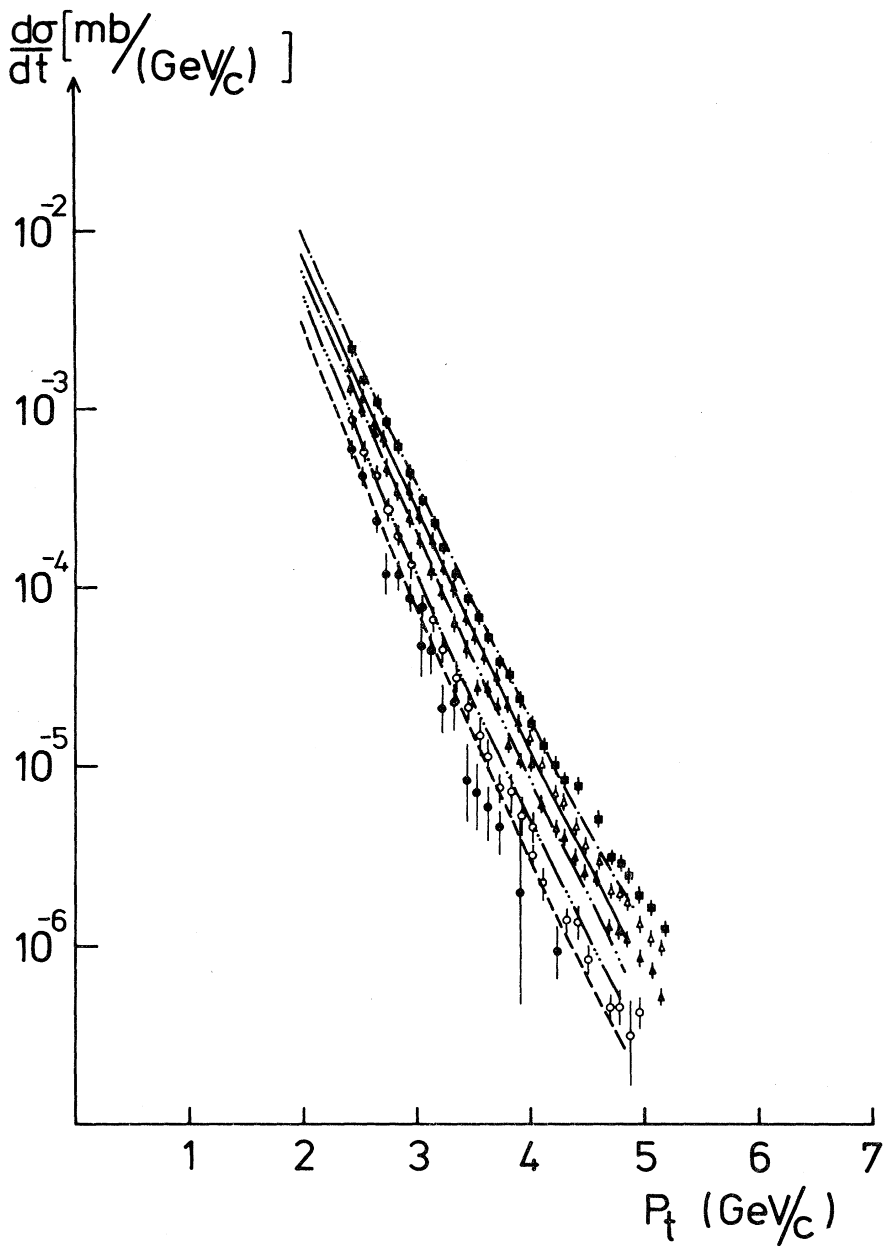

FIG. 3. The inclusive differential cross section of $pp \rightarrow \pi+$anything as a function of transverse momentum P_t. The experimental points (Ref. 7) are solid circle ●, open circle ○, solid triangle ▲, open triangle △, and square □ for $\sqrt{s}=23.5$, 30.6, 44.8, 52.7, and 62.7 GeV, respectively. The various lines are theoretical curves for these respective energies.

$$\sigma_T = 2\int d^2b(1-e^{-\Omega_0}) , \tag{2.12}$$

$$\frac{d\sigma_{\text{el}}}{dt} = \pi \,|\,(1-e^{-\Omega_0})_F\,|^2 . \tag{2.13}$$

The transverse-momentum distribution of an inclusive reaction is

$$\frac{d\sigma}{dk^2} = \text{const} \times \sum_n \left| \left[\frac{\Omega_1{}^n}{n!} e^{-\Omega_0} \right]_F \right|^2 . \tag{2.14}$$

III. COMPARISON WITH DATA

In proton-proton elastic scattering at small momentum transfer $t \lesssim 2$ GeV$^2/c^2$ we can use the simple assumption

$$\Omega_0(b) = \mu_0(F_{1S}{}^2(q^2))_F , \tag{3.1}$$

where $F_{1S}(q^2)$ is the isoscalar form factor of the nucleon. However if we want to take into energy-dependent variation of elastic pp at $t \gtrsim 2$ GeV$^2/c^2$ it is necessary to include the isovector form factor of the nucleon.[6] Similarly we find that in inclusive reactions, it is necessary to in-

TABLE I. Values of parameters.

Total cross section σ_T (mb)	Center of mass $\sqrt{s}$ (GeV)	μ_0	r_S	$\lvert r_V \rvert$	θ
43.11	63	11.5	5.39	3.478	170°
63.73	54.0	19	5.39	3.478	167°
178.73	10^3	26	5.39	3.478	165°
100.75	3×10^3	36	5.39	3.478	160°
39.0	23.5	9.8	5.39	3.478	178°
40.45	30.6	10.3	5.39	3.478	174°
42.05	44.8	10.8	5.39	3.478	172°
43.11	52.7	11.2	5.39	2.478	171°
44.0	62.7	11.5	5.39	3.478	170°

clude the contribution of both isoscalar and isovector form factor in the inelastic transition to explain the larger-momentum-transfer-squared behavior. The assumption is

$$\Omega_1(b)=\mu_0[r_S(F_{1S}{}^2(t))_F+r_V(F_{1V}{}^2(t))_F] , \quad (3.2)$$

where r_S, r_V is the ratio of inelastic transition to elastic transition. The coupling strength μ_0 is determined from the total-cross-section measurement by Eq. (2.4). The r_S, r_V are in general complex, and we let their relative phase be θ:

$$r_V=\lvert r_V\rvert e^{i\theta} ,$$

$$r_S=\text{real} . \quad (3.3)$$

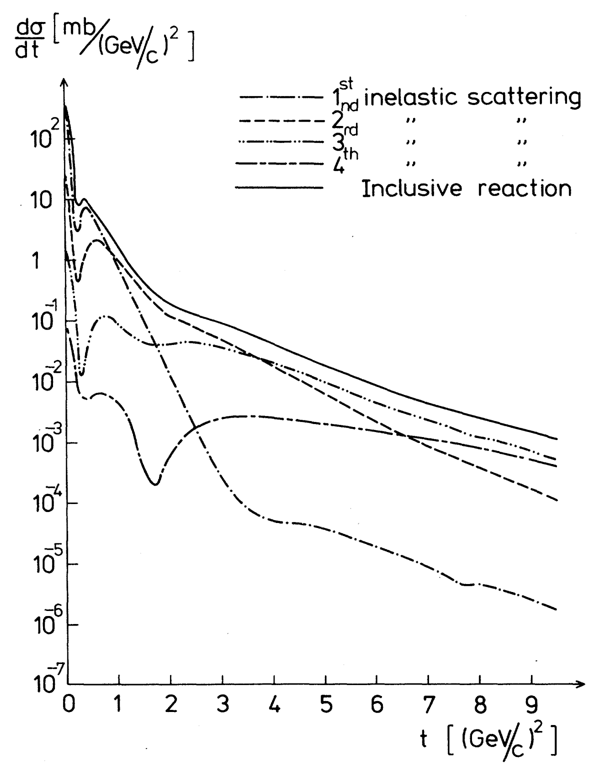

FIG. 4. The composition of inclusive spectrum from various term. The dash-dot curve is for first-order inelastic scattering and the dashed, dash—double-dot, and dashed curves are for second-, third-, and fourth-order inelastic scattering, respectively. The solid curve is the sum total of all the inelastic scattering.

There are no other parameters. Substituting (3.1), (3.2), and (3.3) into (2.7), we obtain the transverse-momentum distribution for $pp\to\pi+$anything. It is shown in Fig. 2. We fit data[7] of $pp\to\pi+$anything at $\sqrt{s}=63$ GeV at 90°, and $\bar{p}p\to\pi+$anything at $\sqrt{s}=540$ GeV. We note the energy dependence comes entirely from the change of values of μ_0 due to the increase of total cross section. The other parameters remain fairly constant. They are listed in Table I. Since there is considerable data on $pp\to\pi+$anything from $\sqrt{s}=23.5$ to 62.7 GeV, we have plotted our fit to these variations in Fig. 3. The parameters used are also listed in Table I. The equation of (2.6) can reproduce all data that span nine decades in magnitude, in the range of $\sqrt{s}=20$ to 540 GeV.

In order to understand the various features of our calculation, we have displayed in Fig. 4 the various terms of $\Omega_1{}^n\exp(-\Omega_0)/n!$ for $n=1,2,3,4$ and show how they add up to produce the curve at $\sqrt{s}=63$ GeV. It is clear from the figure that at $k^2<0.8$ GeV^2/c^2 the first term ($n=1$) dominates. The term itself oscillates just like any diffraction pattern. But as k^2 gets larger, it drops off faster while the $n=2$ term drops off a bit less, and it becomes the dominating term. As one goes to larger and larger k^2 higher and the higher-order term dominates. Since the higher-order term is proportional to $\mu_0{}^n$, it increases like $(\sigma_T)^n$, hence one observes that at larger k^2 the rise of differential cross section is much larger than at smaller k^2.

In Fig. 4 we plot the differential cross section as a function of k^2, the change in slope is more obvious this way. We can roughly see by eye there are three regions $k^2=0$ to 0.3 GeV^2, 0.4 to 2 GeV^2, and 2 to 9 GeV^2 with significant different slopes. We can understand these slope variations as due to the three diffraction peaks coming from the first three terms in the expansion of

$$\frac{\Omega_1{}^n}{n!}\exp(-\Omega_0)=\frac{1}{n!}\left[\Omega_1{}^n-\Omega_1{}^n\Omega_0+\frac{\Omega_1{}^n\Omega_0{}^2}{2!}\cdots\right] .$$

The diffraction pattern, although less obvious than the elastic-scattering case, is still significant. It does not have zeroes because the many terms of different n add up incoherently, but it can explain the flattening off of the slope.

In fact it may be possible to observe clearly such a pattern at higher energy. The terms $\Omega_1{}^n\Omega_0$ become larger, and the kink structure may show up more predominently as we have shown in Fig. 2.

IV. DISCUSSION

(1) It is perhaps instructive to see the actual shape of the isoscalar contribution

$$\frac{\Omega_{1S}{}^n}{n!}\exp(-\Omega_0) \quad (4.1)$$

and the isovector contribution

$$\frac{\Omega_{1V}{}^n}{n!}\exp(-\Omega_0) \quad (4.2)$$

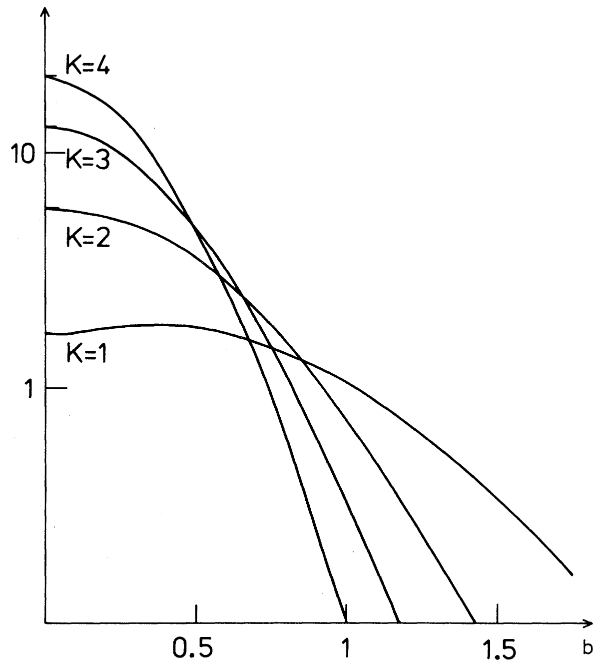

FIG. 5. Isoscalar contribution in the impact-parameter space. We plot $\{[\Omega_K(b)]^K/K!\}e^{-\Omega_0(b)}$ for $K=1,2,3,4$. The larger K is, the more central it is.

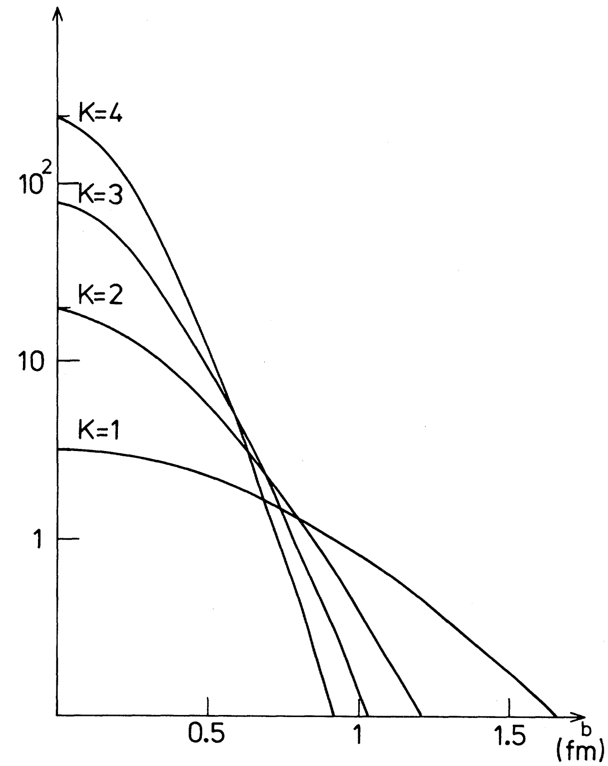

FIG. 6. Isovector contribution in the impact-parameter space. We plot $[(5\Omega_{1V})^K/K!]\exp[-\Omega_0(b)]$ for $K=1,2,3,4$.

in the impact-parameter space, where

$$(\Omega_{1S,V})_F=\mu_0 F_{1S,V}{}^2(k^2)\ . \tag{4.3}$$

These curves are plotted in Figs. 5 and 6 for $n=1,2,3,4$. We notice that qualitatively the isoscalar and isovector contributions are very similar. They differ however numerically. Qualitatively the isovectorial part is smaller at larger b and bigger at smaller b than the isoscalar part. In the momentum space it means the isovector part dominates at larger k^2, and the isoscalar part dominates at smaller k^2. For higher-order terms $n=2$ term peaks more in smaller b than $n=1$ term and $n=3$ term peaks more than $n=2$, etc. Translating to momentum space, smaller-b behavior controls the large-momentum transfer region, just as we have discussed above. Single scattering $(n=1)$ cannot dominate at large k^2 at all.

(2) The invariant cross section of the inclusive reaction

$$E\frac{d^3\sigma}{dp^3}=f(x)g(k^2) \tag{4.4}$$

is assumed to factorize to a function $f(x)$ dependent only on the parallel momentum $(x=p_{11}/p^*)$, and a function $g(k^2)$ dependent on transverse-momentum transfer. Our model here only treats the $g(k^2)$ function. The x dependence must be treated separately.[8]

(3) The original formulation of eikonal model generally requires small-angle scattering. Here we extend it sometimes to 90°, and still find it is close to experimental data. A plausible explanation is that factorization of Eq. (4.4) approximately holds. Therefore it is not critical whether we are concerned with small- or large-angle scattering.

(4) There is always a problem of which form factor to choose in the Chou-Yang model. We have tried all possible combinations in our investigation. Using only Sacks form factor $G_M(q^2)$ or isoscalar form factor alone one cannot fit large-p_t data. One can fit large-p_r data with isovector form factor by itself, but one cannot fit the small-p_t data as well. By trial and error the present fit is the only linear combination that seems to fit all data reasonably well.

(5) We only discuss the pion inclusive spectrum. To discuss the inclusive spectrum of other particles such as K meson, Λ baryon, etc., one needs perhaps to study the particle ratios of these hadrons[9] from the decay of the cluster p^+.

(6) As energy increases the total cross section increases, and the value of μ_0 becomes larger. At any given momentum transfer squared k^2, multiple scattering of higher order becomes more important as energy increases because the nth term increases like $(\mu_1)^n$. For the $\hat{k}^2$ dependence, if the form factor in a single Gaussian $\exp(-\alpha k^2)$, the $\langle \Omega_1{}^n\rangle$ has a dependence of $\exp[-(\alpha/n)k^2]$. Hence as $n\to\infty$ the slope parameter of the $d\sigma/dk^2$ becomes flatter and flatter and approaches zero as a limit. In the limiting case $n\to\infty$ we have a complete flat distribution in k^2 of the differential cross section. We would like to contrast this with the usual argument of QCD where they argue that for large k^2 the result is from single scattering among two quarks, and the differential cross section should behave like $(1/k^2)^2$ for large enough k^2. The geometrical picture here does not necessarily contradict QCD. In fact

the eikonal picture can often be obtained from field theory. The difference is on whether for large k^2 the scattering is dominated by single scattering or multiple scattering. If it is dominated by single scattering the differential cross section probably would eventually have a definite fixed slope at given k^2. However if it is dominated by multiple scatterings, the slope would be continually decreasing as the trend of present data shows.

---

*Permanent address: Institute of High Energy Physics, Academia Sinica, Beijing, P.O. Box 918, China.

[1]T. T. Chou and C. N. Yang, Phys. Rev. D 22, 610 (1980).

[2]T. T. Chou and C. N. Yang, Phys. Rev. Lett. 20, 1213 (1968); M. Kac, Nucl. Phys. B62, 402 (1973); D. J. Clarke and S. Y. Lo, Phys. Rev. D 20, 193 (1979).

[3]S. C. Chan, S. Y. Lo, H. B. Low, and K. K. Phua, Phys. Rev. D 17, 802 (1978); C. H. Lai, S. Y. Lo, and K. K. Phua, Phys. Lett. 122B, 177 (1983); Phys. Rev. D 27, 2214 (1983).

[4]S. Y. Lo, Lett. Nuovo Cimento 2, 124 (1969).

[5]S. Y. Lo, Y. G. Li, and Y. P. Liu, J. High Energy Phys. Nucl. Phys. (China) 5, 653 (1980); S. Y. Lo and Y. G. Li (unpublished).

[6]S. Y. Lo, Nucl. Phys. B7, 286 (1970).

[7]G. Carboni *et al.*, Phys. Lett. 108B, 145 (1982); R. Battiston *et al.*, UA4 Collaboration, *ibid.* 117B, 126 (1982); 115B, 333 (1982); M. Banner *et al.*, UA2 Collaboration, *ibid.* 115B, 59 (1982); D. Drijard *et al.*, CERN-Dortmund-Heidelberg-Warsaw Collaboration, Nucl. Phys. B208, 1 (1982); K. Eggert *et al.*, Nucl. Phys. B98, 49 (1978); F. W. Büsser *et al.*, *ibid* B106, 1 (1976); P. Caliluppi *et al.*, *ibid.* B70, 1 (1974); B79, 189 (1974); A. L. S. Angelis *et al.*, Phys. Lett. 79B, 505 (1978); B. Alper *et al.*, *ibid.* 44B, 521 (1973); W. Akerlof *et al.*, Phys. Rev. D 3, 648 (1971).

[8]See, e.g., M. M. Malone and S. Y. Lo, Phys. Rev. D 16, 2184 (1977); Nuovo Cimento 46, 455 (1978).

[9]C. K. Chew, H. B. Low, S. Y. Lo, and K. K. Phua, J. Phys. G 6, 17 (1980).